

Driving-induced population trapping and linewidth narrowing via the quantum Zeno effect

Charles N. Christensen,^{1,*} Jake Iles-Smith,¹ Torkil S. Petersen,¹ Jesper Mørk,¹ and Dara P. S. McCutcheon²

¹*Department of Photonics Engineering, DTU Fotonik, Ørstedsgade 28, 2800 Kongens Lyngby, Denmark*

²*Quantum Engineering Technology Labs, H. H. Wills Physics Laboratory and Department of Electrical and Electronic Engineering, University of Bristol, BS8 1FD, UK*

(Dated: February 5, 2022)

We investigate the suppression of spontaneous emission from a driven three-level system embedded in an optical cavity via a manifestation of the quantum Zeno effect. Strong resonant coupling of the lower two levels to an external optical field results in a decrease of the exponential decay rate of the third upper level. We show that this effect has observable consequences in the form of emission spectra with subnatural linewidths, which should be measurable using, for example, quantum dot-cavity systems in currently obtainable parameter regimes. These results constitute a novel method to control an inherently irreversible and dissipative process, and may be useful in applications requiring the control of single photon arrival times and wavepacket extent.

The quantum Zeno effect (QZE) refers to a collection of phenomena in which the evolution of a quantum system is inhibited by strong perturbations [1–5]. The first manifestation was coined and popularised by Sudarshan and Misra [5], where the effect is derived as a consequence of frequent projective measurements, i.e. frequent wave function collapses, which are shown to prevent the decay of an otherwise unstable state. Aside from being of general interest to those studying the theory of quantum measurement [6–9], the QZE may also constitute a valuable tool which could be used to inhibit decay and decoherence for quantum information applications [10].

Since the original formulation mentioned above, which proposed to use frequent projective measurements to prevent a dissipative irreversible process, the QZE has since been attributed to other phenomena which deviate from the original in one or both of the following ways. They either 1) use strong *unitary perturbations* in the form of a constant coupling or a sequence of unitary ‘kicks’ [11, 12], and/or 2) they inhibit *coherent dynamics*, as opposed to an incoherent irreversible process [11, 13]. Experimentally, the QZE has been demonstrated in a manner closest to the original proposal in cold atom traps [14, 15], where the incoherent decay of atomic population in a potential well can be inhibited by frequent measurements. The first measurement attributed to the QZE, however, was made by Itano *et al.* [16], who used frequent measurements of a trapped ion to inhibit coherent evolution driven by an rf field, which actually places it in the second of the two categories above, along with those since performed on solid-state spins in diamond [17] and cold atom clouds [18]. Experiments falling into the first category above most notably include dynamical decoupling schemes [19, 20], which make use of sophisticated unitary pulse sequences to prolong coherence times.

Although all of the phenomena discussed above have been referred to as the QZE, it should be understood that the physics involved and potential applicability of each is quite different. In particular, as has long been noted [6–9], the inhibition of *coherent* dynamics by some perturbation requires no notion of wave function collapse, and

can in fact be derived from purely dynamical arguments. Furthermore, from a more practical point of view, there is a significant difference in utility between procedures which inhibit coherent and therefore reversible dynamics, and those which inhibit irreversible decay that may be coherent only on very short timescales [21]. Finally, since the implementation of truly projective measurements has many difficulties it would be highly beneficial if the same ends could be met using unitary couplings.

In this work, we demonstrate how constant strong coherent coupling can inhibit a decay process which is truly irreversible (exponential) on all timescales. Our scheme uses a three-level system embedded in a moderate Q-factor optical cavity, which could be experimentally realised by e.g. a resonantly driven semiconductor quantum dot in a photonic crystal cavity [22–25], as envisaged in Fig. 1 (a). We show that strong driving of the lower two levels results in population trapping in the upper level, which has a clear experimental signature in the form of emission spectra with linewidths which narrow with increasing driving strength. Using realistic parameters, we show that this manifestation of the QZE should be experimentally accessible with current technologies.

Before we begin our detailed analysis, it is instructive to first consider different phenomena which may take place in a three-level system, and how they relate to the QZE. Consider Fig. 1 (b), in which we envisage three equally spaced levels $|g\rangle$, $|e\rangle$ and $|p\rangle$. If states $|p\rangle$ and $|e\rangle$ are coherently coupled, for example with a resonant laser with Rabi frequency Ω_{pe} , a system initially in $|\psi(0)\rangle = |p\rangle$ will evolve into $|\psi(t)\rangle = \cos(\Omega_{pe}t/2)|p\rangle + \sin(\Omega_{pe}t/2)|e\rangle$ [26], with the probability to remain in the initial state given by $|\langle p|\psi(t)\rangle|^2 = \cos^2(\Omega_{pe}t/2)$. If a second field of strength Ω_{eg} is introduced which couples $|g\rangle$ and $|e\rangle$, the probability to remain in the initial state becomes $|\langle p|\psi(t)\rangle|^2 = [(\Omega_{eg}^2 + \Omega_{pe}^2 \cos(\Omega_R t/2))/\Omega_R^2]^2$ with $\Omega_R^2 = \Omega_{pe}^2 + \Omega_{eg}^2$. Evidently, if $\Omega_{eg} \gg \Omega_{pe}$ the transfer of population to $|e\rangle$ is inhibited by the strong coupling of $|e\rangle$ to $|g\rangle$. Although we may refer to such a process as the QZE, since a strong perturbation inhibits a population transfer, it is a consequence of nothing more than the

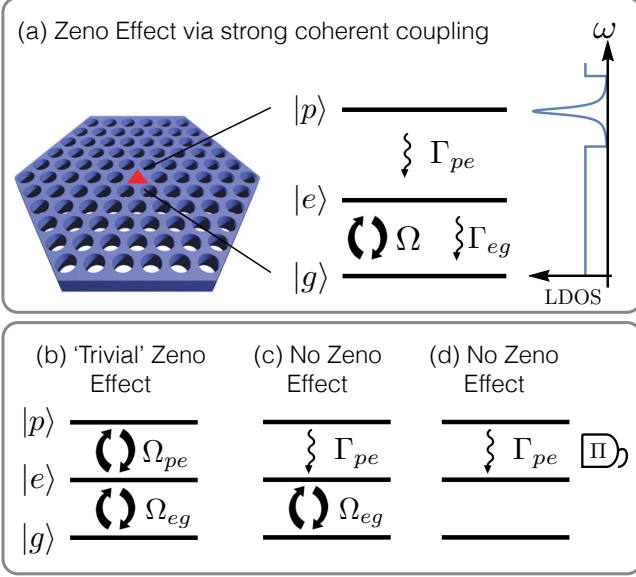


FIG. 1. (a) A three-level system embedded in an optical cavity such that the density of states has a maximum resonant with the bare $|p\rangle \rightarrow |e\rangle$ transition. Strong coherent coupling between the lower two $|e\rangle$ and $|g\rangle$ levels can inhibit population decay from the upper $|p\rangle$ level via a manifestation of the Quantum Zeno Effect. Part (b) shows a similar system with two coherent couplings as shown. When $\Omega_{eg} \gg \Omega_{pe}$ the system exhibits a ‘trivial’ Zeno effect with population residing predominately in $|p\rangle$. Parts (c) and (d) consider a phenomenological incoherent decay process from $|p\rangle$ to $|e\rangle$, with the addition of coherent coupling (c) or rapid projective measurements (d), neither of which give rise to any Zeno effect.

Hamiltonian dynamics of the coupled three levels, having various classical analogues. This simple model highlights the triviality of population trapping or the QZE when referring to the inhibition of a coherent process.

We now consider Fig. 1 (c), in which we replace the coherent interaction between $|p\rangle$ and $|e\rangle$ with a fixed incoherent decay rate Γ_{pe} . One now finds that regardless of any coupling between the lower states, the probability for the excitation to remain in $|p\rangle$ is simply $|\langle p|\psi(t)\rangle|^2 = e^{-\Gamma_{pe}t}$. In contrast to case (b) above, any strong coherent drive no longer affects the rate of population transfer from state $|p\rangle$. Finally, we consider Fig. 1 (d) where projective measurements monitor whether the excitation remains in $|p\rangle$. We wish to calculate the probability that the excitation remains in $|p\rangle$ after a time t , which we now split into N intervals of $\Delta t = t/N$, after each of which we perform a measurement. The probability to find the excitation in $|p\rangle$ for all N measurements is $(|\langle p|\psi(\Delta t)\rangle|^2)^N = (e^{-\Gamma_{pe}\Delta t})^N = e^{-\Gamma_{pe}t}$, which is the same result as before. This simple result demonstrates that projective measurements, no matter how rapid, cannot inhibit a truly exponential decay process.

We will now show how strong continuous coupling can inhibit decay which is modelled as purely exponential with no short-time reversible regime, provided one re-

tains the frequency spectrum of the environment into which the decay takes place. As in the previous cases, we consider a three-level system as in Fig. 1 (a). The lower two levels are driven by a continuous-wave laser of frequency ω_l and Rabi frequency Ω . Rather than modelling the decay processes phenomenologically, we instead couple the three-level system to an electromagnetic environment, modelled as a reservoir of harmonic oscillators. We write the total Hamiltonian as (we set $\hbar = 1$) [27]

$$H = \omega_p |p\rangle\langle p| + \omega_e |e\rangle\langle e| + \Omega \cos(\omega_l t) (\sigma_{eg}^\dagger + \sigma_{eg}) + \sum_{\mathbf{k}} \omega_{\mathbf{k}} b_{\mathbf{k}}^\dagger b_{\mathbf{k}} + \sum_{\mathbf{k}} g_{\mathbf{k}} [(\sigma_{pe}^\dagger + \sigma_{eg}^\dagger) b_{\mathbf{k}} + \text{h.c.}], \quad (1)$$

where ω_e and ω_p are the energies of $|e\rangle$ and $|p\rangle$, $\sigma_{eg} = |g\rangle\langle e|$ and $\sigma_{pe} = |e\rangle\langle p|$, $b_{\mathbf{k}}^\dagger$ is the creation operator for a photon with wavevector \mathbf{k} and frequency $\omega_{\mathbf{k}}$, and we have assumed both $|e\rangle$ and $|p\rangle$ couple to the environment with the same strength $g_{\mathbf{k}}$. Moving into a rotating frame with $T(t) = \exp[i\omega_l(|e\rangle\langle e| + 2|p\rangle\langle p|)t]$ and making a rotating wave approximation we arrive at the Hamiltonian $H'(t) = H_S + H_I(t) + H_E$ where $H_E = \sum_{\mathbf{k}} \omega_{\mathbf{k}} b_{\mathbf{k}}^\dagger b_{\mathbf{k}}$, $H_S = \Delta |p\rangle\langle p| + (\Omega/2)(|e\rangle\langle g| + |g\rangle\langle e|)$, and

$$H_I(t) = \sum_{\mathbf{k}} g_{\mathbf{k}} [(\sigma_{pe}^\dagger + \sigma_{eg}^\dagger) b_{\mathbf{k}} e^{i\omega_e t} + \text{h.c.}], \quad (2)$$

where we have set the laser resonant with the $|g\rangle \rightarrow |e\rangle$ transition, $\omega_l = \omega_e$, and defined $\Delta = \omega_p - 2\omega_l = \omega_p - 2\omega_e$ as the asymmetry in the level spacing.

To proceed we derive a Born–Markov master equation describing the evolution of the three-level system reduced density operator $\rho(t)$, treating $H_I(t)$ as a perturbation to second order. Since our Hamiltonian is time-dependent, in the Schrödinger picture the master equation takes the form [28–30] $\dot{\rho}(t) = -i[H_S, \rho(t)] - \int_0^\infty d\tau \text{Tr}_E [H_I(t), [U_0(\tau) H_I(t-\tau) U_0^\dagger(\tau), \rho(t) \rho_E]]$, where $U_0(\tau) = \exp[-i(H_S + H_E)\tau]$ and ρ_E is the state of the environment, which we take to be the vacuum. Neglecting Lamb shift terms we find we can write the master equation as $\dot{\rho}(t) = -i[H_S, \rho(t)] + \mathcal{D}_{pe}[\rho(t)] + \mathcal{D}_{eg}[\rho(t)]$, where we have made the assumption that electromagnetic fluctuations acting on $|p\rangle$ and $|e\rangle$ are uncorrelated. This is equivalent to coupling each level to identical but independent environments. The first dissipator is

$$\mathcal{D}_{pe}[\rho] = \sum_{\{\eta\}_{pe}} \Gamma(\eta) ([\sigma_{pe}, \rho A_{pe}^\dagger(\eta)] - [\sigma_{pe}^\dagger, A_{pe}(\eta) \rho]), \quad (3)$$

where $A_{pe}(\eta)$ satisfies $U_S(s) \sigma_{pe} U_S^\dagger(s) e^{i\omega_e t} = \sum_{\{\eta\}_{pe}} e^{i\eta s} A_{pe}(\eta)$ and $\sum_{\{\eta\}_{pe}} A_{pe}(\eta) = \sigma_{pe}$, and for this term $\{\eta\}_{pe} = \{\omega_p - \omega_e \pm \Omega/2\}$. The second dissipator is of precisely the same form, but with all occurrences of σ_{pe} replaced with σ_{eg} and the summation running over $\{\eta\}_{eg} = \{\omega_e, \omega_e \pm \Omega\}$. The rates entering these dissipators are equal to the spectral density evaluated at these specific frequencies, $\Gamma(\eta) = \pi \sum_{\mathbf{k}} g_{\mathbf{k}}^2 \delta(\omega_{\mathbf{k}} - \eta)$. For emission into a continuum of modes, $\Gamma(\eta)$ is taken

to be a smooth function proportional to the density of photonic environment states [24].

Before this is explored in more detail, we can already see how optical driving of the lower $|e\rangle$ and $|g\rangle$ states can give rise to population trapping and the QZE, since the master equation rates depend on the driving strength Ω through the summation in Eq. (3). Using the master equation we find $\rho_{pp} = \langle p|\rho|p\rangle$ satisfies $\dot{\rho}_{pp} = -\Gamma_{pe}\rho_{pp}$ with $\Gamma_{pe} = \Gamma(\omega_p - \omega_e + \Omega/2) + \Gamma(\omega_p - \omega_e - \Omega/2)$. It is evident that for a flat spectral density the driving strength does not affect the decay of population from $|p\rangle$. For spectral densities with non-trivial frequency dependence, however, driving the lower two levels can affect the rate at which population leaves the upper $|p\rangle$ state.

To illustrate this, we consider a spectral density that describes that of a photonic crystal cavity, consisting of a Lorentzian resonance inside a background optical density of states (DOS) with a photonic band gap [31, 32]. The Lorentzian contribution is given by [24] $\Gamma_{\text{cav}}(\omega) = g^2(\kappa/2)[(\omega - \omega_c)^2 + (\kappa/2)^2]^{-1}$, where κ and ω_c are the cavity width and central frequency, while g is the emitter-cavity coupling strength. Away from the cavity the DOS is assumed flat, giving a background rate Γ_B . The composite frequency-dependent emission rate is therefore

$$\Gamma(\omega) = \begin{cases} \Gamma_{\text{cav}}(\omega), & |\omega - \omega_c| \leq (1/2)\xi, \\ \Gamma_B, & \text{otherwise.} \end{cases} \quad (4)$$

with ξ the width of the photonic band gap. One can see that if the cavity is chosen to be on resonance with the bare $|p\rangle \rightarrow |e\rangle$ transition, i.e. $\omega_p - \omega_e = \omega_c$, then as the driving strength increases from $\Omega = 0$ to $\kappa < \Omega < \xi$ both rates entering Eq. (3) will become suppressed.

Our model demonstrates that spontaneous emission from the upper level can be inhibited by strongly driving the lower two levels. To investigate experimental signatures of this phenomenon, we now consider the emission spectrum of the complete system, and for concreteness use parameters which correspond to experimentally achievable regimes for quantum dots in photonic crystal cavities [22–24]. For this system the states $|e\rangle$ and $|p\rangle$ could be formed by the exciton and biexciton respectively, with the level spacing asymmetry Δ then corresponding to the biexciton binding energy [33]. We envisage initialising the system in $|p\rangle$, driving the lower two levels, and observing the frequency spectrum of all emitted light. We note that some care must be taken to choose an appropriate time interval over which to measure, since the emitted field will be neither stationary nor vanishing in the long time limit. We therefore consider the time-dependent spectrum defined as [34, 35]

$$R(\Delta\omega, t) = \text{Re} \left[\int_0^t ds \int_0^{t-s} d\tau g^{(1)}(s, \tau) e^{(\nu - i\Delta\omega)\tau} e^{-2\nu(t-s)} \right],$$

where ν is the resolution of the spectrometer, assumed to be Lorentzian, and $g^{(1)}(t, \tau) = \langle E^\dagger(t + \tau)E(t) \rangle$ is the first-order field correlation function with $E^\dagger(t)$ the

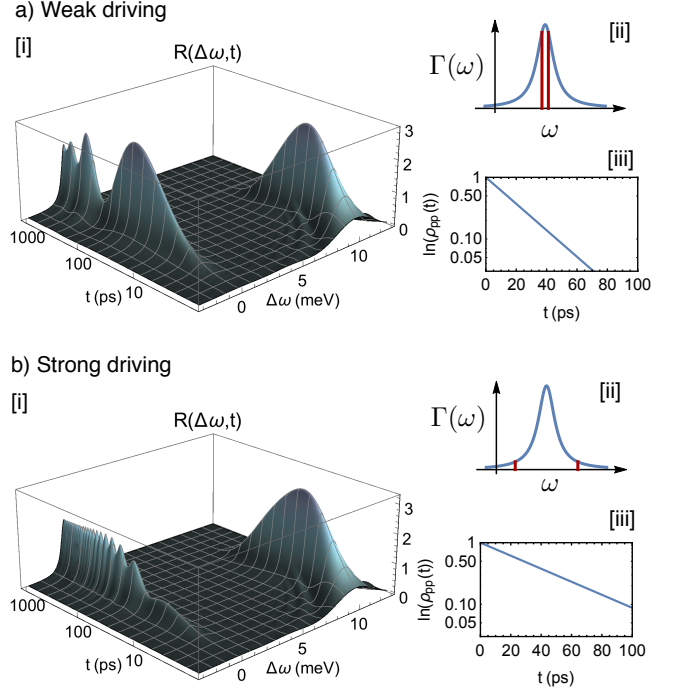


FIG. 2. Parts [i] show time-dependent emission spectra for a three-level system initially in the upper state $|p\rangle$, where the driving between the lower two levels is (a) weak ($\Omega = 10 \mu\text{eV}$) and (b) strong ($\Omega = 100 \mu\text{eV}$). For stronger driving, emission from the lower subsystem is delayed, due to a decrease in the emission rates for the upper system, as indicated by the red lines in [ii], and shown explicitly by the population dynamics of the $|p\rangle$ level in [iii]. Parameters: $\Delta = 10 \text{ meV}$, $\kappa = 0.1 \text{ meV}$, $\Gamma_B^{-1} = 500 \text{ ps}$, $[2\Gamma_{\text{cav}}(\omega_c)]^{-1} = (4g^2/\kappa)^{-1} = 20 \text{ ps}$ and $\nu^{-1} = 2 \text{ ps}$.

positive frequency component of the electric field. The time-dependent spectrum is a generalisation of the usual Wiener-Khinchin theorem suitable for non-stationary fields and guaranteed to be positive [34–36]. The correlation function is calculated by making the identification $E^\dagger(t) \propto \alpha\sigma_{eg}(t) + \beta\sigma_{pe}(t)$ with α and β constants, and can then be calculated using our master equation and the quantum regression theorem [27, 29, 34].

We first consider the case in which the bandwidth of the spectrometer is rather broad compared to typical spectral features of the driven three-level system, corresponding to the condition $\nu > \Gamma(\omega)$, Ω , the benefit being that the spectrometer can temporally resolve the system dynamics. In Fig. (2) we show time-dependent spectra for a spectrometer resolution of $\nu^{-1} = 2 \text{ ps}$, for weak (a) and strong (b) driving, where the bare $|p\rangle \rightarrow |e\rangle$ transition is $\Delta = 10 \text{ meV}$ larger than the $|e\rangle \rightarrow |g\rangle$ transition, and resonant with the cavity. The spectra show an initial delay of $\sim 1 \text{ ps}$ due to ‘filling’ of the spectrometer [34], giving way to emission from $|p\rangle$ seen by the peak around $\Delta\omega = 10 \text{ meV}$. This is then followed by emission from $|e\rangle$ seen around $\Delta\omega = 0$, in which damped Rabi oscillations can be resolved. Comparing (a) and (b), one can see

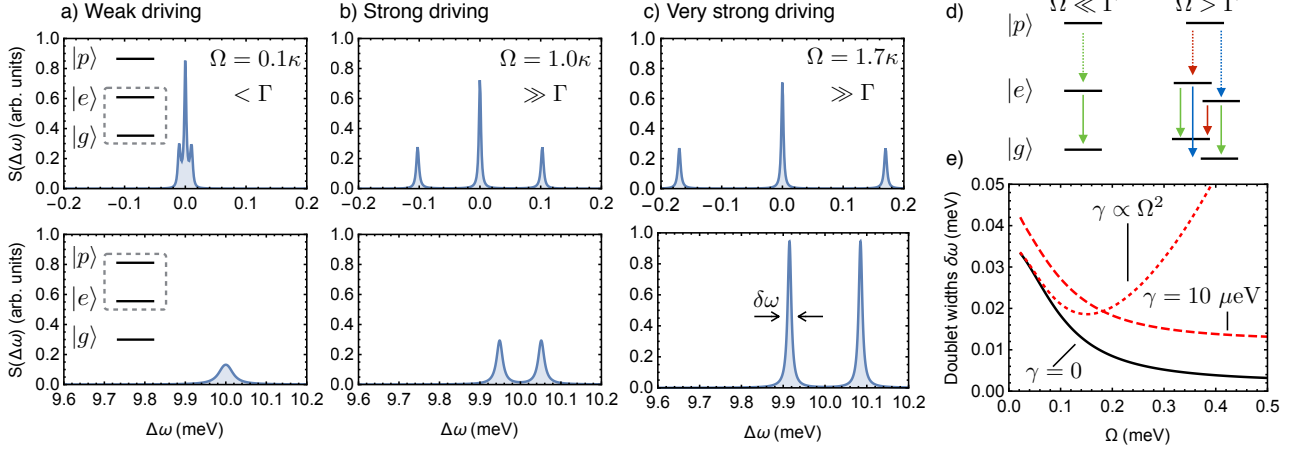


FIG. 3. Parts (a)–(c) show time-integrated emission spectra for weak ($\Omega = 10 \mu\text{eV}$), strong ($\Omega = 100 \mu\text{eV}$) and very strong ($\Omega = 170 \mu\text{eV}$) driving strengths, with the two rows showing features around $\Delta\omega = 0$ and $\Delta\omega = 10$ meV, pertaining to the two subsystems as indicated. The driving hybridises eg -subsystem into dressed states as depicted in (d), which then splits the $|p\rangle$ emission line into a doublet, whose peaks then narrow with increasing Ω , as seen by the solid curve in (e). The red dashed curve in (e) shows the effect of a constant pure-dephasing term, while the red dotted curve corresponds to a driving-dependent dephasing term as expected for excitons in quantum dots. Here $\nu = 0.3 \mu\text{eV}$ and all other parameters as in Fig. (2).

that stronger driving introduces a greater delay before emission from $|e\rangle$ is observed. This is because the rates dictating decay of the $|p\rangle$ level decrease, as indicated by the red lines in parts [ii], and also seen explicitly in parts [iii] which show the population dynamics.

Time-domain spontaneous emission suppression is perhaps the most intuitive way the QZE may be observed, though reproducing time-dependent spectra or population dynamics is rather challenging. To avoid this, we now consider the case where $\nu \ll \Gamma, \Omega$. In this limit the spectrometer is able to resolve detailed spectral features, but provides little timing resolution, and it is therefore more appropriate to consider the time-integrated spectrum $S(\Delta\omega) = \int_0^T dt R(\Delta\omega, t)$ for $T \gg \nu^{-1}$. This is what would be typically measured experimentally when using a high-resolution Fabry-Perot interferometer.

In Fig. 3 (a)–(c) we show time-integrated spectra for increasing driving strengths as indicated, for a spectrometer with realistic resolution $\nu = 0.3 \mu\text{eV} = 2\pi \times 67 \text{ MHz}$ [37, 38], and an integration time of $T = 3 \text{ ns}$. With this increased spectral resolution, we can now see that the driving causes the emission peak from the $|p\rangle$ level to split into a doublet, while simultaneously the spectral features around $\Delta\omega = 0$ pertaining to the lower two levels display a Mollow triplet. As depicted in Fig. 3 (d), the driving hybridises the lower two levels into dressed states, giving the upper $|p\rangle$ level two decay paths of differing energies. These paths sample the spectral density away from its peak centred at the bare undressed $|p\rangle \rightarrow |e\rangle$ transition energy, and have correspondingly suppressed rates. The suppression of the rates with increased driving strength, which can be considered the QZE, here manifests as a narrowing of the emission lines. This narrowing is clearly seen in Fig. 3 (e), where the

solid black curve shows the doublet peak linewidths $\delta\omega$ as a function of driving strength.

Also shown in Fig. 3 (e) is the behaviour of the doublet linewidths when dephasing is present, obtained by adding a term $2\gamma(|e\rangle\langle e|\rho|e\rangle\langle e| - (1/2)\{|e\rangle\langle e|, \rho\})$ to the master equation defined above Eq. (3), and shown by the dashed red curve. For the specific case of excitons in quantum dots, excitation-induced dephasing caused by coupling to phonons is expected to give a driving-dependent dephasing rate $\gamma \approx \pi\alpha k_B T \Omega^2$ [27, 37]. For a realistic exciton-phonon coupling constant of $\alpha = 0.03 \text{ ps}^2$ and temperature of $T = 4 \text{ K}$ we obtain the dotted red curve. Importantly, due to the quadratic nature of driving dependence, a clear reduction in the doublet peak width is still observed, after which the dephasing overwhelms the suppression of spontaneous emission and the peaks begin to broaden. We note, however, that in this regime spontaneous emission is still suppressed.

We have shown that strong driving of a three-level system in an optical cavity can give rise to spontaneous emission suppression via a manifestation of the quantum Zeno effect. Experimental signatures of this effect may be seen in the narrowing of emission lines with increasing driving strength, which should be observable even in the presence of dephasing processes. Though framed in terms of quantum dots, our results are rather general, and could be used to control the temporal extent or arrival times of photons for quantum information applications.

J.I.-S. and J.M. acknowledge support from the Danish Research Council (DFF-4181-00416) and Villum Fonden (NATEC Centre). This project has received funding from the European Union's Horizon 2020 research and innovation programme under the Marie Skłodowska-Curie grant agreement No. 703193.

* Corresponding author: charles.n.chr@gmail.com

- [1] P. Facchi and S. Pascazio, J. Phys. A Math. Theor. **41**, 493001 (2008).
- [2] Y.-R. Zhang and H. Fan, Sci. Rep. **5**, 11509 (2015).
- [3] W. M. Itano, J. Phys. Conf. Ser. **196**, 012018 (2009).
- [4] P. Facchi, G. Marmo, and S. Pascazio, Journal of Physics: Conference Series **196**, 1 (2009).
- [5] B. Misra and E. C. G. Sudarshan, J. Math. Phys. **18**, 756 (1977).
- [6] T. Petrosky, S. Tasaki, and I. Prigogine, Physics Letters A **151**, 109 (1990).
- [7] E. Block and P. R. Berman, Phys. Rev. A **44**, 1466 (1991).
- [8] S. Pascazio and M. Namiki, Phys. Rev. A **50**, 4582 (1994).
- [9] L. E. Ballentine, Phys. Rev. A **43**, 5165 (1991).
- [10] G. A. Paz-Silva, A. T. Rezakhani, J. M. Dominy, and D. A. Lidar, Phys. Rev. Lett. **108**, 080501 (2012).
- [11] S. Pascazio and P. Facchi, Phys. Rev. A (2003).
- [12] S. Pascazio, P. Facchi, and D. A. Lidar, Phys. Rev. A **69**, 032314 (2004).
- [13] S. Pascazio and P. Facchi, Phys. Rev. Lett. **89**, 080401 (2002).
- [14] M. C. Fischer, B. Gutiérrez-Medina, and M. G. Raizen, Phys. Rev. Lett. **87**, 040402 (2001).
- [15] Y. S. Patil, S. Chakram, and M. Vengalattore, Phys. Rev. Lett. **115**, 140402 (2015).
- [16] W. M. Itano, D. J. Heizen, J. J. Bollinger, and D. J. Wineland, Phys. Rev. A **41**, 2295 (1989).
- [17] J. Wolters, M. Strauß, R. S. Schoenfeld, and O. Benson, Phys. Rev. A **88**, 020101 (2013).
- [18] F. Schäfer, I. Herrera, S. Cherukattil, C. Lovecchio, F. S. Cataliotti, F. Caruso, and A. Smerzi, Nature Comms. **5**, 3194 (2014).
- [19] L. Viola and S. Lloyd, Phys. Rev. A **58**, 2733 (1998).
- [20] L.-A. Wu and D. A. Lidar, Phys. Rev. Lett. **88**, 207902 (2002).
- [21] K. Koshino and A. Shimizu, Phys. Rev. Lett. **92**, 030401 (2004).
- [22] D. Englund, D. Fattal, E. Waks, G. Solomon, B. Zhang, T. Nakaoka, Y. Arakawa, Y. Yamamoto, and J. Vučković, Phys. Rev. Lett. **95**, 013904 (2005).
- [23] K. Hennessy, A. Badolato, M. Winger, D. Gerace, M. Atature, S. Gulde, S. Falt, E. L. Hu, and A. Imamoglu, Nature **445**, 896 (2007).
- [24] K. Roy-Choudhury and S. Hughes, Phys Rev B **92**, 205406 (2015).
- [25] K. Roy-Choudhury and S. Hughes, Opt. Lett. **40**, 1838 (2015).
- [26] D. Walls and G. Milburn, *Quantum Optics* (Springer, 2008).
- [27] A. Nazir and D. P. S. McCutcheon, J. Phys. Condens. Matter **28**, 103002 (2016).
- [28] H. P. Breuer and F. Petruccione, *The Theory of Open Quantum Systems* (Oxford University Press, Oxford, 2002).
- [29] D. P. S. McCutcheon, Phys. Rev. A **93**, 022119 (2016).
- [30] K. Roy-Choudhury and S. Hughes, Optica **2**, 434 (2015).
- [31] T. Suhr, N. Gregersen, K. Yvind, and J. Mørk, Opt. Express **18**, 11230 (2010).
- [32] T. Suhr, N. Gregersen, M. Lorke, and J. Mørk, Applied Physics Letters **98**, 211109 (2011).
- [33] F. Hargart, M. Müller, K. Roy-Choudhury, S. L. Portalupi, C. Schneider, S. Höfling, M. Kamp, S. Hughes, and P. Michler, Phys. Rev. B - Condens. Matter Mater. Phys. **93**, 115308 (2016), arXiv:1509.03861.
- [34] J. H. Eberly and K. Wódkiewicz, J. Opt. Soc. Am. **67**, 1252 (1977).
- [35] A. Moelbjerg, P. Kaer, M. Lorke, and J. Mørk, Phys. Rev. Lett. **108**, 017401 (2012).
- [36] E. del Valle, A. Gonzalez-Tudela, F. P. Laussy, C. Tejedor, and M. J. Hartmann, Phys. Rev. Lett. **109**, 183601 (2012).
- [37] Y.-J. Wei, Y. He, Y.-M. He, C.-Y. Lu, J.-W. Pan, C. Schneider, M. Kamp, S. Höfling, D. P. S. McCutcheon, and A. Nazir, Phys. Rev. Lett. **113**, 097401 (2014).
- [38] S. Ulrich, S. Ates, S. Reitzenstein, A. Löffler, A. Forchel, and P. Michler, Phys. Rev. Lett. **106**, 247402 (2011).